*33rd EPS Conference on Plasma Phys. Rome, 19 - 23 June 2006 ECA Vol.**30I**, P-2.001 (2006)*

Stopping of Calcium ions in low density SiO_2 aerogels

A.D. Fertman[1], T.Yu. Mutin[1], V.I. Turtikov[1], A. Blazevic[2], V.P. Efremov[3], A.A. Golubev[1], D.H.H. Hoffmann[2,4], S. Korostiy[4], S.A. Pikuz jr.[3], O.N. Rosmej[2], B.Yu. Sharkov[1],

[1] ITEP, Moscow, Russia; [2] GSI, Darmstadt, Germany; [3] IHED RAS, Moscow, Russia;

[4] TU Darmstadt, Germany

During last years we have investigated the stopping processes of heavy ions in condensed matter using K-shell radiative transitions of energetic ions penetrating solid targets for determination of the projectile charge state and velocity along the ion beam trajectory. The method description and experimental results have been presented in [1-3]. The use of low-density aerogel targets in the experiments instead of quartz increased the ion stopping range by a factor 5–100 and gave the possibility to visualize the dynamics of the projectile radiation along the ion trajectory. In this paper the results of experimental investigation of the possible influence of the aerogel porous nanostructure on the ion stopping process are presented. The measured energy loss and the mean equilibrium charge of the 11.4 MeV/u ^{48}Ca ions interacting with Al foils and aerogel targets with approximately the same linear densities ρx are compared with each other and with calculations using SRIM code [4] and various empirical formulas [5-8].

In experiments on the interaction of heavy ion beams with solid matter carried out at UNILAC accelerator at GSI, SiO_2 aerogels and aluminium foils were used as a target material. Non-organic aerogel with densities in the range of 0.02 - 0.5 g/cm^3 is a special, highly porous solid substance with very low density [9]. It is characterized by higher heat resistivity than usual solid SiO_2, lower thermal conductivity and can withstand temperatures up to 750 C without damage. The gel structure is formed by chains of colloidal SiO_2 beads of 3 nm in diameter. The chains of beads build the 3D opened cell structure, like a sponge, with pores less than 30 – 50 nm in diameter. The dimensions and weight of aerogel targets have been measured in GSI Target laboratory [10], in that way the linear density of targets fabricated at the Institute for Catalysis RAS Novosibirsk was controlled (Table 1).

The linear density of the aluminium foils used in experiments was in the range of 6.9 – 17.0 mg/cm^2. They were supplied by GSI Target Laboratory. The accuracy of the foil-thickness was estimated to be 10 μg/cm^2.

For energy loss measurements a time-of-flight method (TOF) was used. This method is based on a strongly resonant way of the ion beam accelerating in RFQ linac that leads to a

certain phase correlation between the beam microstructure and the accelerating RF-voltage structure (~ 108 MHz sinus for our case) in any point of a beam-line including the target position and stop detector position [11]. A stop detector consisting mainly of a micro-sphere plate (working similar as a micro-channel plate, rise time: 150 ps [12]) was placed at the end of the 473 cm long time-of-flight path after the target. Experimental scheme is presented in Fig. 1a. The stop detector signal and the UNILAC RF-signal were recorded simultaneously using a digital oscilloscope (sample rate 2.5 GS/s). When the ion beam penetrates the target a phase shift of the beam microstructure relatively to the RF signal occurs due to the ion energy loss in stopping media. Together with an accurately measured target – detector distance (TOF distance) this shift gives a difference between the initial ion velocity and the velocity after the beam passed through the target. This procedure allows the determination of the ion energy loss in the target.

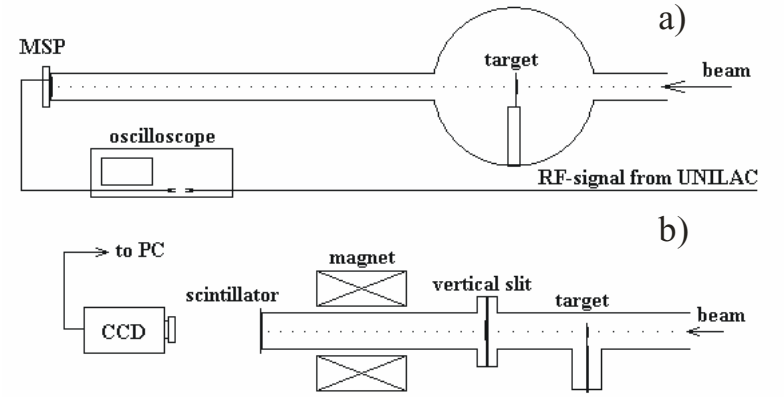

Fig. 1. Experimental setup for the measurements of the energy loss and charge state distribution of the ion beam

As a result, 11.4 MeV/u Calcium beam energy losses in aerogel and aluminium targets have been determined. The experimental results are summarized in Table 1.

Table 1. Energy losses of 11.4 MeV/u Ca ions in SiO_2 aerogel and Al targets

Target/ Density g/cm^3	Linear density, mg/cm^2	Energy loss, MeV/u		Mean charge state (experiment)
		experiment	SRIM2003.26	
Al	6.9	1.57±0.06	1.558	18.79±0.07
Al	12	2.88±0.08	2.812	18.52±0.07
Al	13.81	3.14±0.08	3.283	18.5±0.07
Al	16.98	4.17±0.06	4.15	18.22±0.07
Aerogel/0.023	7.02	1.69±0.09	1.77	18.54±0.07
Aerogel/0.019	12.0	3.06±0.08	3.16	18.28±0.07
Aerogel/0.048	13.6	3.38±0.08	3.635	18.25±0.07
Aerogel/0.023	19.3	4.91±0.06	5.44	17.82±0.07

New experimental data on the stopping power for fast ions are traditionally compared with the values predicted by the publicly available SRIM code [4]. We also present such a comparison in Table 1. One can see that our experimental results on the Ca ion energy loss

in Al targets are in good agreement with SRIM 2003 values, and the discrepancy of experimental and calculated energy loss values in aerogels does not exceed 12 %.

For measuring the charge-states of heavy ions after passing through target foils one usually uses special setups including magnetic analysis of ions according to their charge- states [13,14] or broad-range magnetic analyzers [13,16]. The setup used in the present work for the measurement of the charge-state distributions of ^{48}Ca ions accelerated at the UNILAC accelerator is schematically presented in Fig. 1b. For the analysis of charge state distribution after interaction with the investigated target, the beam burst is deflected in the B=1–1.8 T magnetic field of a dipole magnet. The deflection of different ion charge states are realized according to their charge-to-mass ratio Q/m and energy. The ion impacts were detected by a plastic scintillator (1 mm thick), viewed by a camera which produces intensified images on a charge coupled device (CCD). The background picture of the foreign lighting and CCD noise was registered and subtracted for each image. Afterwards, the images were projected along the direction of the dispersion. Since the beam energy after the target is known from the TOF measurements, the charge state distribution of the ion beam can be determined. Figure 2 shows the charge state distribution of the Ca ion beam with initial energy of 11.4 MeV/u after penetration Al foil and the aerogel target of approximately the same linear density.

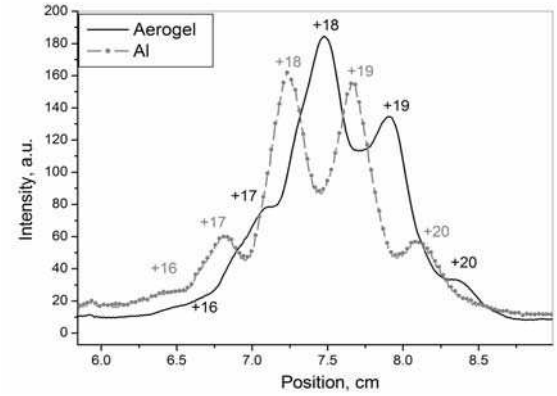

Fig. 2. The profiles of the ^{48}Ca beam image after analyzing magnet: black - charge state distribution after passing through the Al foil with a linear density of 13.8 mg/cm^2; grey - after penetration of the 0.048 g/cm^3 aerogel target with a linear density of 13.6 mg/cm^2.

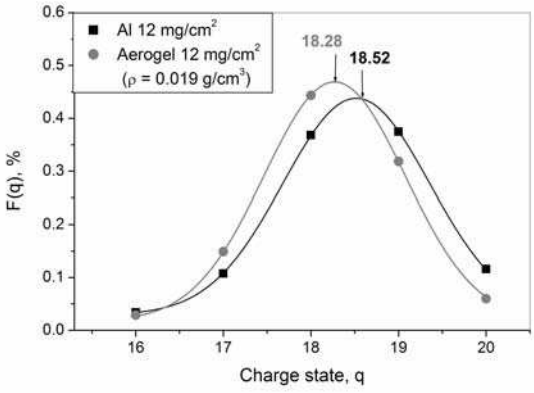

Fig. 3. Charge-state distributions of ^{48}Ca ions at 11.4 MeV/u after passing through an Al foil (E = 8.52 Mev/u) and a aerogel sample (E = 8.34 Mev/u). The experimental data are approximated with a Gaussian functions.

There are several approaches based on Bohr's criterion [15], which are used to estimate the average equilibrium charge of heavy ions ($\bar{q}$) and the distribution of the charge-state fractions F(q) of the ion beam when heavy ions with atomic number Z, charge q and velocity v pass through a certain material thick enough for them to attain charge

equilibration – a detailed presentation of this can be found in the review articles [5,13]. The mean charge $\bar{q}$ is defined as $\bar{q} = \sum_q q \cdot F(q)$. For practical cases the charge-state distribution of heavy ions emerging from a solid target is approximated with a Gaussian curve [17]. Charge-state distributions of ^{48}Ca ions at 11.4 MeV/u after passing through an Al foil (E_{out} = 8.52 Mev/u) and a aerogel sample (E_{out} = 8.34 Mev/u) are presented on Fig. 3. These results suggest that at our experimental conditions the pore of 30-50 nm sizes does not seriously influence the ion stopping processes. Other experimental results are summarized in Table 1.

Measured average charge states of Ca ions in comparison with calculations using different semi-empirical formulas [5 – 8] are presented in Fig. 4. The semi-empirical formula of Schiwietz provides the best coincidence with experimental data.

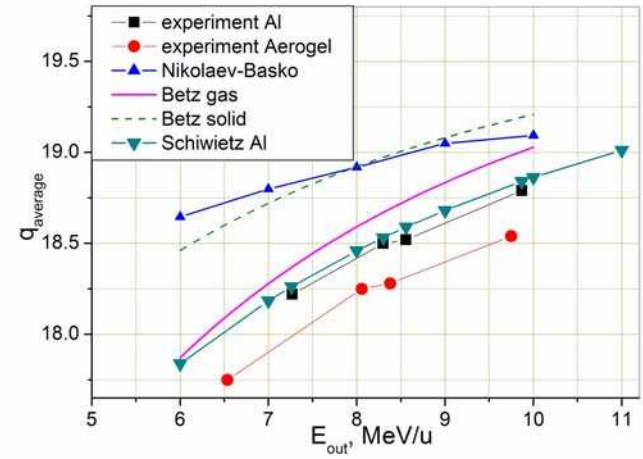

Fig. 4. Average charge state of $^{48}Ca^{7+}$ ions after propagation through Al and aerogel targets.

The financial support of this work from WTZ project 670 and from the CRDF BRHE program (REC-011-Y2-P-11-04 Fellowship), is gratefully acknowledged

REFERENCES

1. O. N. Rosmej *et al.*, Nucl. Instrum. Methods Phys. Res. A 495, (2002) 2;
2. O. N. Rosmej *et al.*, Laser Part. Beams 23, (2005) 79;
3. O. N. Rosmej *et al.*, Physical Review A 72, (2005) 052901;
4. J.F. Ziegler SRIM-2003, www.srim.org;
5. Betz, H.D., Rev. Mod. Phys., 44 (1972), 465;
6. V.S. Nikolaev, I.S. Dmitriev, Phys. Lett. A 28, (1968) 277;
7. M. Basko, Sov. J. Plasma Phys. 10 (1984) 689;
8. G. Schiwietz, P.L. Grande Nucl. Instrum. Methods Phys. Res. B 175 - 177 (2001) 125–131;
9. N.G. Borisenko, Ya.A. Merkuliev, Targets having microheterogeneous structure for the spherical laser compression, Proceedings of P.N. Lebedev Institute, Vol. 221, Nova Science Publishers, New York, 1996;
10. H. Folger, A Nucl. Instrum. Methods Phys. Res. A 438 (1999) 131-151;
11. A. D. Fertman, T. Yu. Mutin, M. M. Basko et al Nucl. Instrum. Methods Phys. Res. B 247 (2006) 199;
12. MSP Technical data, El-Mul Technologies Ltd, http://www.tectra.de/e/Detect.htm
13. N.K. Skobelev, Phys. Part. Nucl. 20 (1989) 1439 (in Russian);
14. W. Liu, G. Imbriani, L. Buchmann, et al., Nucl. Instrum. Methods Phys. Res. A 496 (2003) 198;
15. V.Z. Maidikov, Yu.V. Gofman, G.S. Popeko, N.K. Skobelev, Prib. Tech. Exp. 4 (1979) 68;
16. N. Bohr, Phys. Rev. 58 (1940) 654; N. Bohr, Phys. Rev. 59 (1941) 270.
17. K. Shima, T. Mikumo, H. Tawara, At. Data Nucl. Data Tables 34 (1986) 357;